

Mold Wear during Permanent-Mold Casting of Ti-6Al-4V

P.A. Kobryn, R. Shivpuri, and S.L. Semiatin

(Submitted 22 December 2000; in revised form 7 March 2001)

Mold wear during the casting of Ti-6Al-4V in a permanent (steel) mold was investigated using a combination of macro- and micro-scale observations and measurements. For this purpose, a steel mold with interchangeable inserts of three candidate mold steels (H13, P20, and 1040) was used. Inserts were removed at regular intervals during casting under prototype-production conditions and inspected to assess mold wear. Two major mold wear types were identified: soldering and "wrinkling." Soldering was concluded to be a result of local over-heating of the mold, and wrinkling a result of cyclic stresses caused by a combination of solid-state phase transformations and large temperature gradients. The 1040 inserts performed the best; soldering was less severe and wrinkling did not occur. The better performance of the 1040 inserts was attributed to lower mold temperatures and thermal gradients due to the higher thermal conductivity of 1040 relative to H13 or P20.

Keywords H13 steel, mold wear, P20 steel, permanent mold casting, Ti-6Al-4V, type 1040 steel

1. Introduction

Permanent-mold casting (PMC) is a well-known casting technique in which a component is made by pouring liquid metal into a reusable metal mold. The method is frequently used for the casting of aluminum alloys. In this case, the molds are typically made of steel. Advantages over sand or investment casting include the elimination of processing steps (because the mold can be reused) and the refinement of as-cast grain size, a result of faster cooling.

Recently, the application of PMC to the casting of titanium alloys has been investigated.[1] Titanium PMC provides a means of producing relatively complex parts with close tolerances and finer grain sizes. In comparison to investment casting of titanium, Ti PMC requires fewer processing steps, greatly reduces the size of alpha case, and eliminates the risk of ceramic inclusions. Therefore, the process is extremely attractive to the aerospace industry. However, the Ti PMC process has several key challenges, which are not of concern for conventional PMC. For instance, to prevent contamination of the molten titanium, Ti PMC must be performed in an inert atmosphere and special skull-melting techniques must be employed. Additionally, because titanium melts at around 1700 °C and is extremely reactive, Ti PMC molds see much higher temperatures and a more extreme environment than conventional PMC molds.

Determination of mold life is particularly critical to the development and eventual implementation of Ti PMC inasmuch as mold life has a tremendous impact on cost. Hence, mold wear is a critical area for Ti PMC research. While no Ti PMC research results can be found in the literature, numerous researchers have investigated die wear during die casting of various nontitanium alloys.[2–6] These researchers found various wear types, the most common being soldering, washout/erosion/abrasion, corrosion, and heat checking. The specific type and extent of wear were found to depend upon variables such as casting alloy, mold material, and mold temperature history. Based on these results and the major differences between Ti PMC and conventional metal-mold casting, research to determine the types and extent of wear that occur during Ti PMC is needed.

The present work was undertaken to determine the wear characteristics of three candidate mold steels: the hot-work tool steel H13, which is commonly used for aluminum die-casting dies and hot forging dies; the mold steel P20, which is commonly used for plastic injection-molding molds and zinc die-casting dies; and the plain-carbon steel 1040, which is comparatively inexpensive and easy to work and machine. The performance of the three steels was assessed *via* a combination of visual and dimensional inspection and microstructural characterization. The results were used to determine wear mechanisms and to guide the selection of future mold materials.

2. Approach

2.1 Materials

The materials used in this investigation consisted of Ti-6Al-4V melt stock and H13 tool steel, P20 tool steel, and 1040 plain-carbon steel for the mold and six sets of mold inserts. The Ti-6Al-4V had a composition (in wt.%) of 6.52 aluminum, 4.18 vanadium, 0.2 iron, 0.0298 carbon, 0.221 oxygen, 0.012 nitrogen, 23.5 ppm hydrogen, balance titanium. The H13 tool steel had a composition of 0.40 carbon, 0.28 manganese, 0.96 silicon, 5.10 chromium, 1.24 molybdenum, 0.81 vanadium, 0.15 nickel, 0.049 copper, 0.004 sulfur, balance iron. The P20 tool steel had a composition of 0.30 carbon, 0.80 manganese, 0.30 silicon, 1.10 chromium, 0.55 molybdenum, 0.08 vanadium, 0.015 phosphorus, 0.003 sulfur, balance iron. The 1040 plain carbon steel had a composition of 0.47 carbon, 0.75 manganese, 0.25 silicon, and balance iron.

P.A. Kobryn and **S.L. Semiatin,** Air Force Research Laboratory, Materials and Manufacturing Directorate, AFRL/MLLMP, Wright-Patterson AFB, OH 45433; and **R. Shivpuri,** Department of Industrial, Welding, and Systems Engineering, The Ohio State University, Columbus, OH 43210. Contact e-mail: pamela.kobryn@afrl.af.mil.

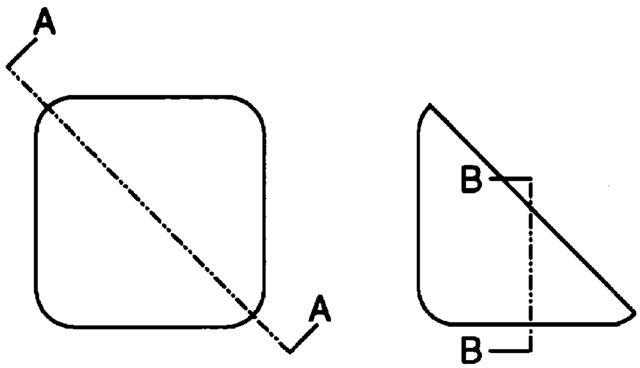

Fig. 1 Top views of a mold insert showing the two cross-sections used for metallography

A proprietary casting-evaluation mold designed and fabricated by Howmet Corporation (Whitehall, MI) was used for this investigation. The design included mold *inserts* which could be readily removed between casting trials. Six sets of mold inserts (consisting of one insert of each material) were fabricated. The corner/edge radii on the inserts in the first four sets were 3.18 mm, while those in the remaining two sets were 4.76 and 6.35 mm, respectively. Prior to casting, the H13 mold inserts possessed a fine tempered-martensite microstructure with a hardness of R_C 47 to 51, the P20 inserts a coarser bainitic structure with a hardness of R_C 23 to 24, and the 1040 inserts a hot-rolled ferrite-plus-pearlite structure with a hardness of R_C 16.

2.2 Casting Trials

Melting and casting trials were conducted to establish the wear characteristics of the three steels. All trials were performed using the vacuum-arc-melting system located at Howmet's Operhall Research Center. For the first pour, the first set of inserts was installed in the mold. After making a single casting, these inserts were removed from the mold and replaced with new ones. In a similar fashion, a total of 6, 12, 75, 75, and 75 pours were made on sets 2 through 6, respectively. The sets onto which 75 pours were made were removed incrementally for non-destructive evaluation after 12 and 37 pours.

2.3 Insert Characterization

Following removal from the mold, the inserts were visually inspected. Photographs were taken and the mass and bulk hardness of each insert were measured. Additionally, select insert dimensions were measured using a programmable coordinate-measurement machine (CMM) after 37 and 75 pours on sets 4 through 6. The composition of the surface of selected inserts was measured at critical locations using a scanning electron microscope (SEM) equipped with an electron dispersive spectroscopy (EDS) system.

After non-destructive characterization, the inserts were sectioned and prepared for microscopy using conventional metallographic techniques. Two cross-sections from each were prepared: a diagonal cross-section through one corner of the insert (the "triple corner") and a perpendicular cross-section through one side of the insert (the "double corner") (Fig. 1). The microstructures of the cross-sections were examined and photographed using an optical microscope equipped with a digital image-capture system. The hardness of critical areas of selected insert cross-sections was also measured using a microhardness tester equipped with a precision-controlled motorized stage. A Vicker's diamond pyramid indenter was used at 300 g for 5 s, and traverses were performed from the corners inward at a variable interval dependent on the local hardness. The composition of selected cross-sections was measured at critical locations using a SEM equipped with a wavelength dispersive spectroscopy (WDS) system. Traverses were performed from the corners inward at a spacing of 5 μm.

2.4 Analysis of Mold-Insert Characterization Results

The photographs, micrographs, and EDS results were analyzed to qualitatively evaluate changes in the appearance, microstructure, and composition of the inserts, respectively, while the mass, hardness, CMM, and WDS results were analyzed to quantitatively evaluate changes. Results were used to assess mold-material durability and to identify active mold-wear mechanisms.

3. Results and Discussion

The principal results of this investigation comprised the qualitative assessment of macroscopic mold-wear characteristics and surface composition; the quantitative assessment of macroscopic changes in mass, hardness, and dimensions; the qualitative assessment of microstructural changes; and the quantitative assessment of microscopic changes in hardness and chemical composition. These results were used to draw conclusions about potential wear types and the underlying mechanisms.

3.1 Macroscopic Inspection Results

Visual Inspection Results. The main observations regarding mold wear of steel inserts during PMC of Ti-6Al-4V are illustrated in Fig. 2 and may be summarized as follows.

- A shiny "solder" appeared on the insert triple corners even after one pour.
- The remaining surface area appeared duller and somewhat rougher than the precasting surface.
- The shiny solder area grew as more pours were made.
- The solder area was largest on the H13 inserts and smallest on the 1040 inserts.
- The triple corners rounded off and wore away as more pours were made.
- The double corners of the H13 and P20 inserts started to "wrinkle" as more pours were made.
- The double corners rounded off slightly as more pours were made.
- The triple corners rounded off much more quickly than the double corners.
- The flat faces did not appear to wear at all.

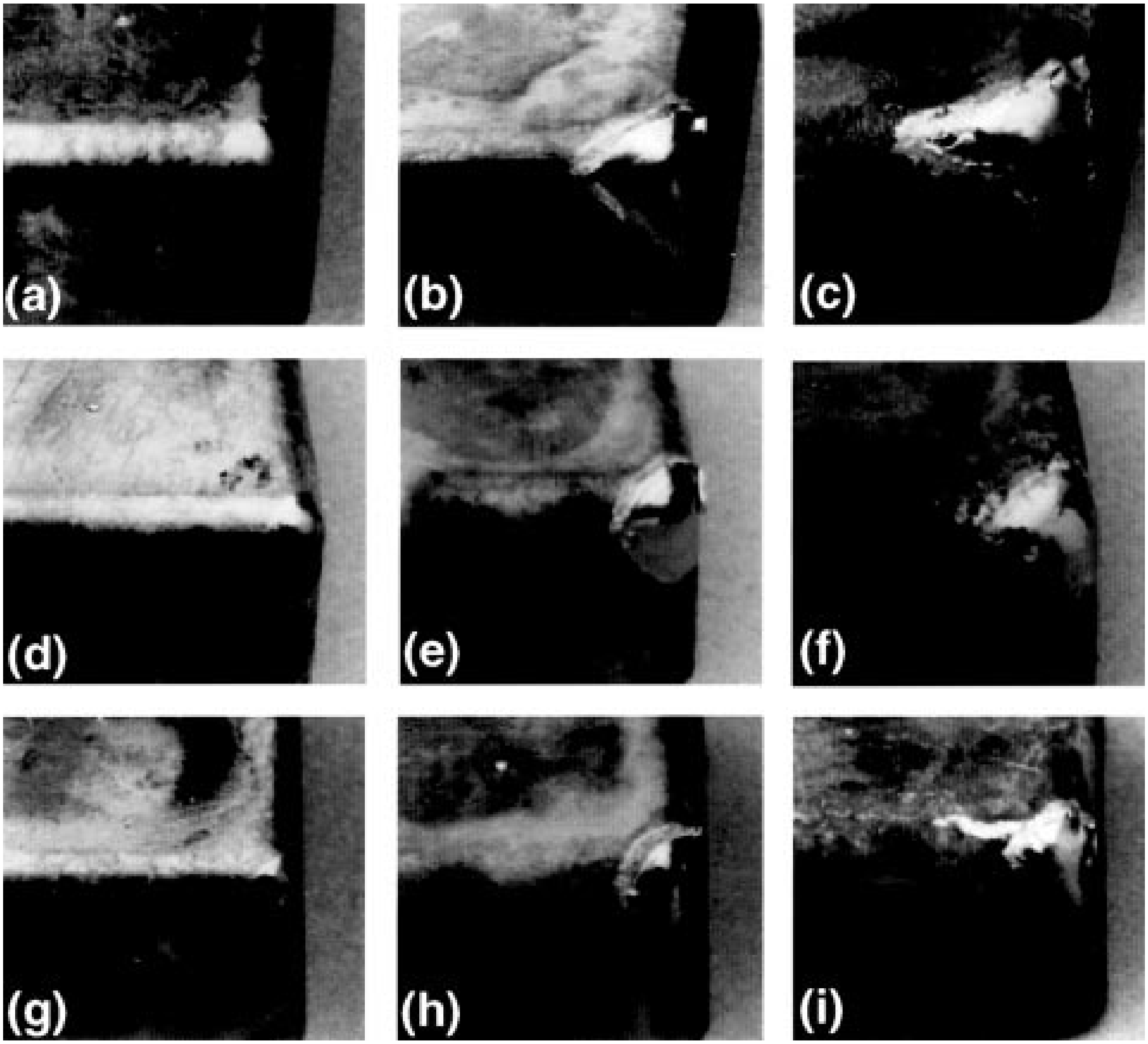

Fig. 2 Photographs of corner regions of (**a**) to (**c**) H13, (**d**) to (**f**) P20, and (**g**) to (**i**) 1040 mold inserts after (**a**), (**d**), and (**g**) 1 pour, (**b**), (**e**), (**h**) 12 pours, and (**c**), (**f**), (**i**) 75 pours

Based on these observations, two important wear types were identified: soldering and wrinkling (Fig. 3). The observed shininess of the surface of the solder layer indicated that the solder was in the liquid phase at the time of mold-insert retraction, and, hence, was a solidification product. The appearance of the surface of the wrinkled regions was similar to that of the rest of the insert, indicating that the wrinkles were formed in the solid state. Both soldering and wrinkling were investigated in detail *via* microscopic inspection to determine the underlying mechanisms (Sections 3.3 and 3.4).

Mass Measurement Results. The mass of all of the mold inserts decreased as more pours were made on them. While the 1040 and P20 inserts lost between 0.1 and 0.2 g over 75 pours, the H13 blocks lost between 0.2 and 0.6 g. These results are summarized in Fig. 4(a), in which the change in mass is plotted for each insert. Error bars, indicating the limits of a pooled *t*-test 5% confidence interval, were so close together that they fell within the symbols. Because the initial mass of each of the inserts was nearly identical, these results indicate that H13 wore more rapidly than the other two materials.

Hardness Measurement Results. The bulk hardnesses of all of the inserts decreased by approximately 3 points on the R_C scale over the course of 75 pours. These results are summarized in Fig. 4(b), in which the change in hardness is plotted for each insert and the error bars indicate the limits of a pooled *t*-test 5% confidence interval. These results indicate that all of the materials softened slightly as more pours were made.

CMM Measurement Results. The CMM results were analyzed to determine the average thickness of material lost in each of three locations on the mold inserts: the triple corners, the double corners, and the flat faces (Table 1). These measurements indicated that the triple corners wore significantly more than

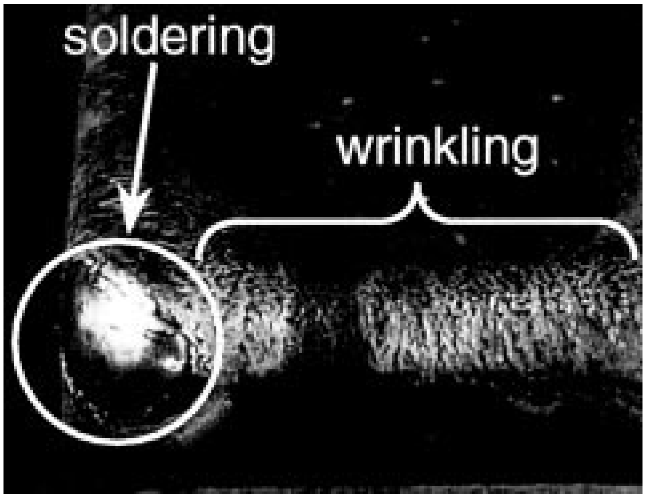

Fig. 3 Photograph of a P20 mold insert after 37 pours of Ti-6Al-4V, illustrating the soldering and wrinkling wear types

either the double corners or the flat faces, as expected. The H13 triple corners wore more rapidly than the P20 triple corners, which wore more rapidly than the 1040 triple corners. The results also indicated that the double corners of the 1040 and P20 inserts wore the same amount, while the H13 double corners did not wear as much. However, due to the wrinkling on the P20 and H13 double corners, these results are not necessarily an accurate measure of material loss. The results from the flat faces were similar for all three materials, as the average measured losses for each were within less than 1.5 standard deviations of one another. The effect of varying the corner/edge radius was not clear due to scatter in the data. However, because all three radii resulted in appreciable wear, the threshold radius must be larger than the largest radius tested.

EDS Measurement Results. EDS was performed on the surface of selected inserts immediately after they were removed from the mold. Data were collected from the flat faces, double corners, and triple corners. The results from the flat faces and the double corners were very similar (Fig. 5a). In both cases, the spectra had very large aluminum peaks with smaller but significant titanium peaks and very small peaks from the elements present in the base steel. For the triple corners, the titanium peaks were the largest, followed by the iron and aluminum peaks (Fig. 5b). In all cases, the composition did not appreciably vary locally. Based on these results and the visual inspection results, it is likely that the apparently Al-rich layer found on the majority of the insert surface was deposited from the Al-rich vapor that forms during the vacuum-melting process, while the apparently Ti-rich layer on the triple corners was formed from the liquid state during casting.

3.2 Microscopic Inspection Results: General Insert Microstructure

Visual Inspection Results. The postcasting mold-insert microstructures near the double and triple corners were significantly different from the initial microstructures (Fig. 6). In all three materials, the microstructures at and just below the surface of the corners were much finer than the original microstructures,

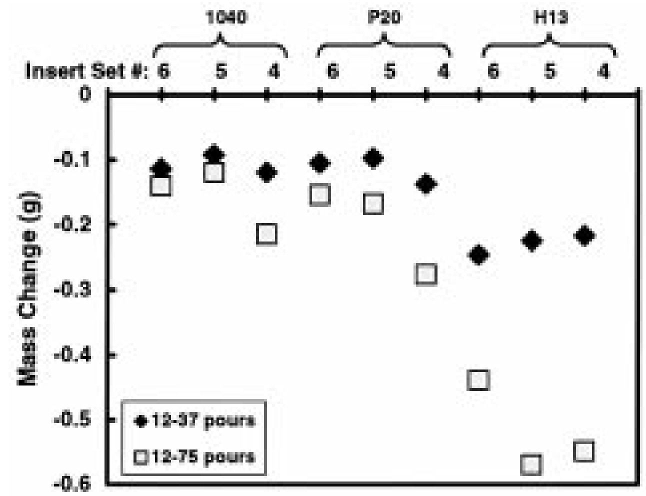

(**a**)

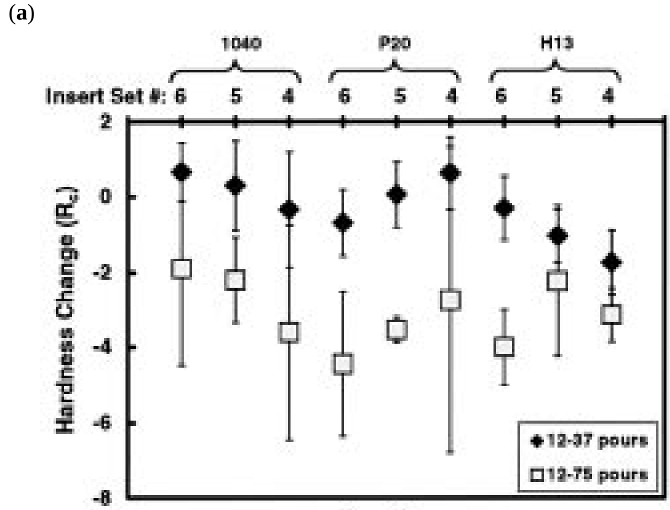

(**b**)

Fig. 4 Plots of changes in (**a**) mass and (**b**) hardness of H13, P20, and 1040 mold inserts from 12 to 75 pours of Ti-6Al-4V

Table 1 Mold insert dimensional losses from 37 to 75 pours

Material	Insert set	Triple corners	Double corners	Flat faces
1040	4	0.074 mm	0.048 mm	0.056 mm
1040	5	0.064 mm	0.041 mm	0.051 mm
1040	6	0.099 mm	0.056 mm	0.038 mm
	1040 average:	0.079 mm	0.048 mm	0.048 mm
P20	4	0.135 mm	0.079 mm	0.053 mm
P20	5	0.180 mm	0.043 mm	0.038 mm
P20	6	0.155 mm	0.020 mm	0.033 mm
	P20 average:	0.157 mm	0.048 mm	0.041 mm
H13	4	0.239 mm	0.025 mm	0.043 mm
H13	5	0.246 mm	0.013 mm	0.025 mm
H13	6	0.130 mm	0.013 mm	0.028 mm
	H13 average:	0.206 mm	0.015 mm	0.033 mm

while the structures further away from the surface appeared to be overtempered/annealed. As described in Ref 7, these changes indicate that the temperature of the inserts in these regions

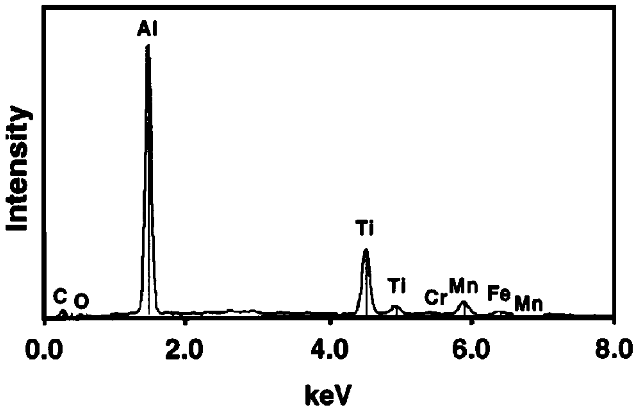

(**a**)

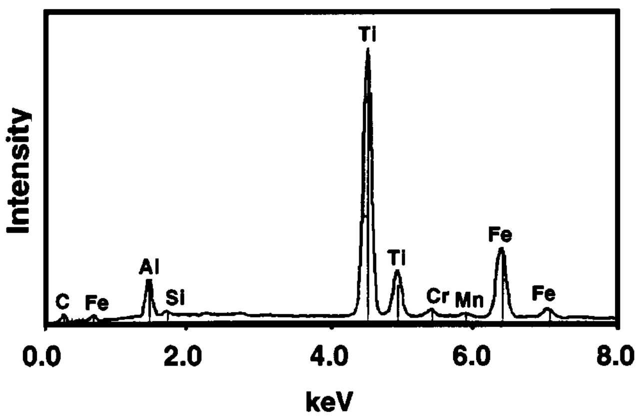

(**b**)

Fig. 5 EDS spectra from the surface of an H13 mold insert after 75 pours of Ti-6Al-4V from (**a**) a double corner and (**b**) a triple corner

reached values high enough to cause complete or partial austenitization near the surface and significant overtempering/annealing further away from the surface.

Microhardness Measurement Results. The results of microhardness traverses from the triple and double corners inward confirmed the visual interpretation of the microstructures. Just beneath the corner surfaces, the hardnesses were higher than the pre-casting hardnesses, while further away from the corner surfaces, the hardnesses were lower than the precasting hardnesses (Fig. 7). This result indicated that the material closest to the surface reached the lower critical temperature (at a minimum) and formed a harder structure upon cooling, while the material further away reached a peak temperature *below* the lower critical temperature and was overtempered/annealed.

The microstructure and microhardness results were combined to determine the depth of the overtempered/annealed and/or austenitized regions in the double and triple corners. Using these depths and the corresponding transformation temperatures (as calculated from the compositions using the equations in Ref 8), the minimum peak temperatures and thermal gradients developed within the triple-corner transformation zones during casting were calculated (Table 2). These results showed that the peak temperatures in the 1040 triple corners were up to 165 °C lower than those in the H13 and up to 55 °C lower than those in the P20 triple corners. The results also showed that the thermal gradients in the 1040 triple corners were likely significantly lower than those in either the H13 or P20 triple corners. These results are as expected, as the thermal conductivity of the 1040 inserts is, in general, significantly higher than that of the H13 or P20 inserts.[9] Hence, 1040 would be expected to be more resistant than P20 or H13 to any type of wear directly related to peak temperature and/or thermal gradient.

3.3 Microscopic Inspection Results: Soldering

Visual Inspection Results. In addition to the aforementioned transformation zones, the triple-corner solder layer was also easily identified under the microscope. Upon etching with Nital, a clearly visible layer of ferrite (the lightly colored phase in the micrograph) was found at the interface between the solder layer and the base steel (Fig. 8), indicating that carbon had diffused from the insert into the solder layer. However, no structure was visible in the solder layer itself, indicating that it consisted of a phase (or multiple phases) for which Nital was not a viable etchant. Upon etching with Vilella's reagent, a typical etchant for martensitic steel, virtually no structure was evident in the solder layer as well (Fig. 9a), indicating that the solder did not consist of martensite. However, upon re-etching with Kroll's reagent, a typical titanium etchant, the structure of the solder layer became clearly visible (Fig. 9b), indicating that the solder layer likely consisted primarily of titanium. This result is consistent with the macroscopic results reported in Section 3.1.

WDS Measurement Results. WDS results revealed that the composition of the solder near the surface of the triple corners was approximately 60% titanium, 30% iron, and 10% other elements by weight (Fig. 10a). Moving toward the center of the insert, there was an abrupt change in composition resulting in a composition of approximately 1.5% titanium, 88.5% iron, and 10% other elements by weight, after which the titanium composition decreased smoothly to approximately zero (Fig. 10b).

Based on these results, the solder was concluded to consist of a titanium-rich layer separated from the base steel by a diffusion layer slightly enriched with titanium. As reported previously,[7] conclusions regarding the probable solder phases and their formation temperatures were drawn from the Ti-Fe phase diagram.[10] The relative amounts of titanium and iron in the solder layer indicated that the composition was near that of the Ti-TiFe eutectic, which has a melting temperature of 1085 °C. Because of the abrupt change in composition between the solder layer and the underlying diffusion layer, it is likely that the surface of the mold-insert triple corner melted during casting, allowing the liquid steel to mix locally with the liquid titanium. Due to its low melting temperature, the solder adhered to the surface of the mold insert because it was still in the liquid state at the time the insert was retracted. Hence, solder formation was likely driven by the peak temperature of the mold surface. This hypothesis is supported by the comparative severity of soldering on the three materials, with the relatively hot H13 inserts being more severely soldered than the relatively cool 1040 inserts.

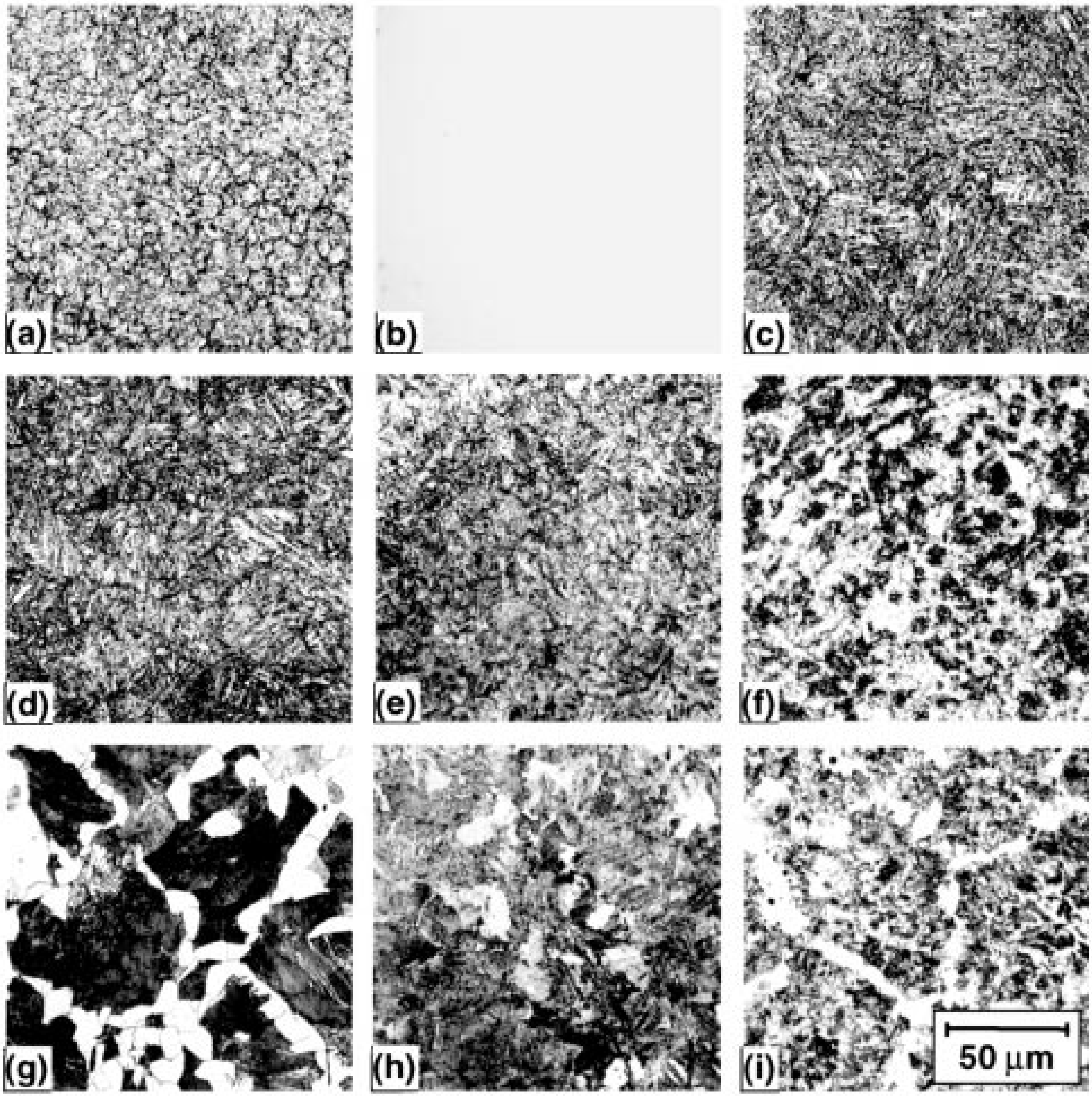

Fig. 6 Micrographs of (**a**) to (**c**) H13, (**d**) to (**f**) P20, and (**g**) to (**i**) 1040 mold inserts showing (**a**), (**d**), (**g**) the triple-corner microstructure before casting and after 75 pours at locations (**b**), (**e**), (**h**) several microns below the surface, and (**c**), (**f**), (**i**) several millimeters below the surface (Nital etch; note: (**b**) appears blank because Nital does not etch 100% untempered martensite)

3.4 Microscopic Inspection Results: Wrinkling

Visual Inspection Results. The double-corner wrinkling could not be observed using the original two sections of the mold inserts, so a new section was cut perpendicular to the wrinkles. In this specimen, the wrinkles appeared as smooth undulations in the surface of the insert (Fig. 11). In addition to the smooth undulations in the surface, a discrete, uniform layer of an unknown material was visible at the surface of this double corner. The layer was approximately 8 μm in thickness and was continuous over the surface of the specimen. The shape and periodicity of the undulations did not appear to scale with any features of the surface layer or any microstructural features of the steel, indicating that the wrinkling likely was *not* caused by a microstructure- or composition-related phenomenon (such as selective melting, diffusion, or erosion).

Based on these results, the wrinkle-formation mechanism was concluded to be a type of thermal fatigue resulting from the stresses induced during repeated heating and cooling of the

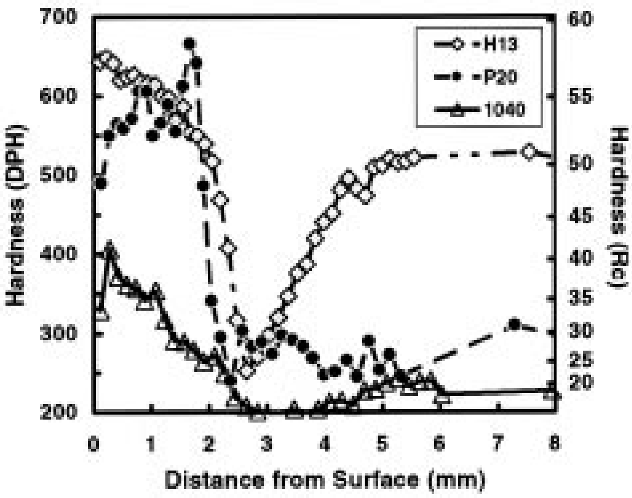

(**a**)

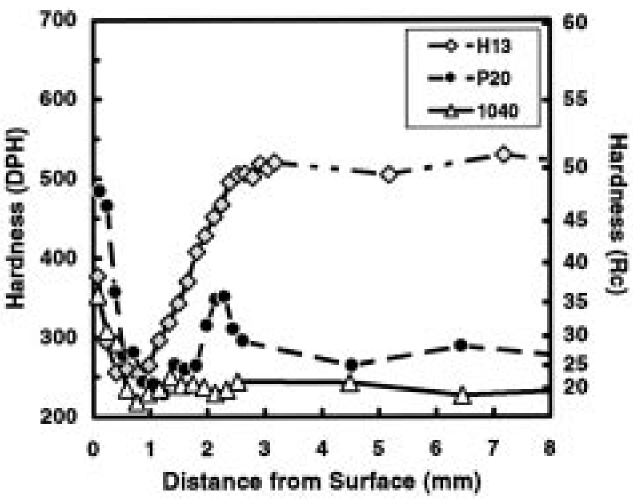

(**b**)

Fig. 7 Microhardness measurements from sections through H13, P20, and 1040 mold inserts following 75 Ti-6Al-4V pours: (**a**) triple corners and (**b**) double corners

Table 2 Transformation-zone properties of mold-insert triple corners

Material	Ac_1 temperature (°C)	Minimum hardness depth (mm)	Ac_3 temperature (°C)	Full hardness depth (mm)	Minimum *dT/dx* (°C/mm)
H13	834	2.6	947	1.9	161
P20	741	2.3	838	1.8	194
1040	722	2.8	782	0.0	21

mold inserts. In conventional thermal fatigue of die-casting or forging dies, an array of orthogonal cracks called "heat checks" forms due to repeated non-uniform thermal expansion and contraction.[2] The severity of heat checking increases with increasing thermal stresses, which, in turn, increase with increasing

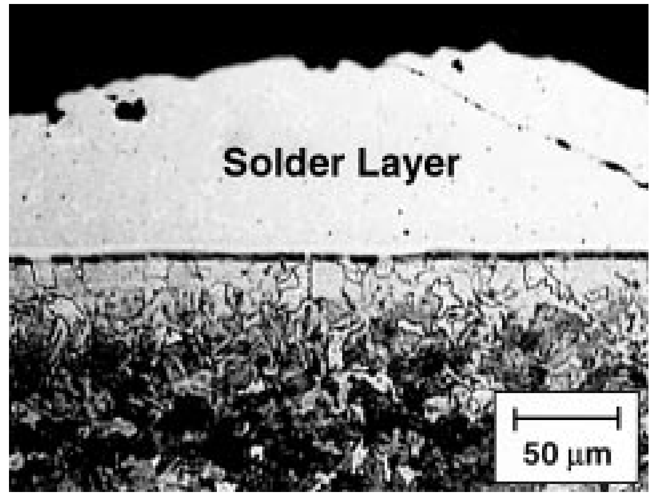

Fig. 8 Micrograph of the surface of a triple corner from a 1040 mold insert showing the solder layer and the carbon-depleted region in the steel (Nital etch)

thermal gradients. In the case of Ti PMC, a similar but more extreme thermal expansion/contraction cycle would result because of the volume change due to phase transformations. However, because of the high temperatures involved, it is possible that the induced thermal stresses are relieved by plastic deformation, resulting in wrinkle formation instead of cracking. Hence, wrinkle formation was likely driven by both the peak temperatures *and* the thermal gradients near the double-corner surfaces, with the peak temperatures controlling the volume of material which transformed and the thermal gradients determining the magnitudes of the thermal stresses. This hypothesis is supported by the comparative severity of wrinkling on the three materials, with the relatively hot, high-gradient H13 and P20 inserts wrinkling severely and the relatively cool, low-gradient 1040 inserts showing no wrinkling at all.

WDS Measurement Results. WDS results revealed that the composition approximately 10 μm below the surface of the double corners was ~3% aluminum, 0.5% titanium, 88% iron, and 8.5% other elements (Fig. 12). (Unfortunately, accurate WDS data could not be obtained closer to the surface.) Within 15 μm of the surface, there was an abrupt change in aluminum composition, after which the percentage of aluminum decreased to approximately zero in the bulk of the insert. The percentage of titanium dropped off more smoothly, reaching zero by approximately 25 μm. As the percentage of aluminum and titanium decreased, the percentage of iron and chromium increased, as expected.

These results, when combined with the macroscopic inspection results, give credence to the hypothesis that an Al-rich layer was deposited on the surface of the mold from the vapor phase during melting. Because there was a significant amount of titanium in the Al-rich layer, it would have been possible for the layer to survive during casting (inasmuch as the melting point of a binary Al-Ti alloy containing as little as 10 wt.% Ti is 1200 °C,[11] which, in turn, is much higher than the expected peak surface temperature of the double corners[7]). Based on these results, compositional variations do not appear to play a role in wrinkling.

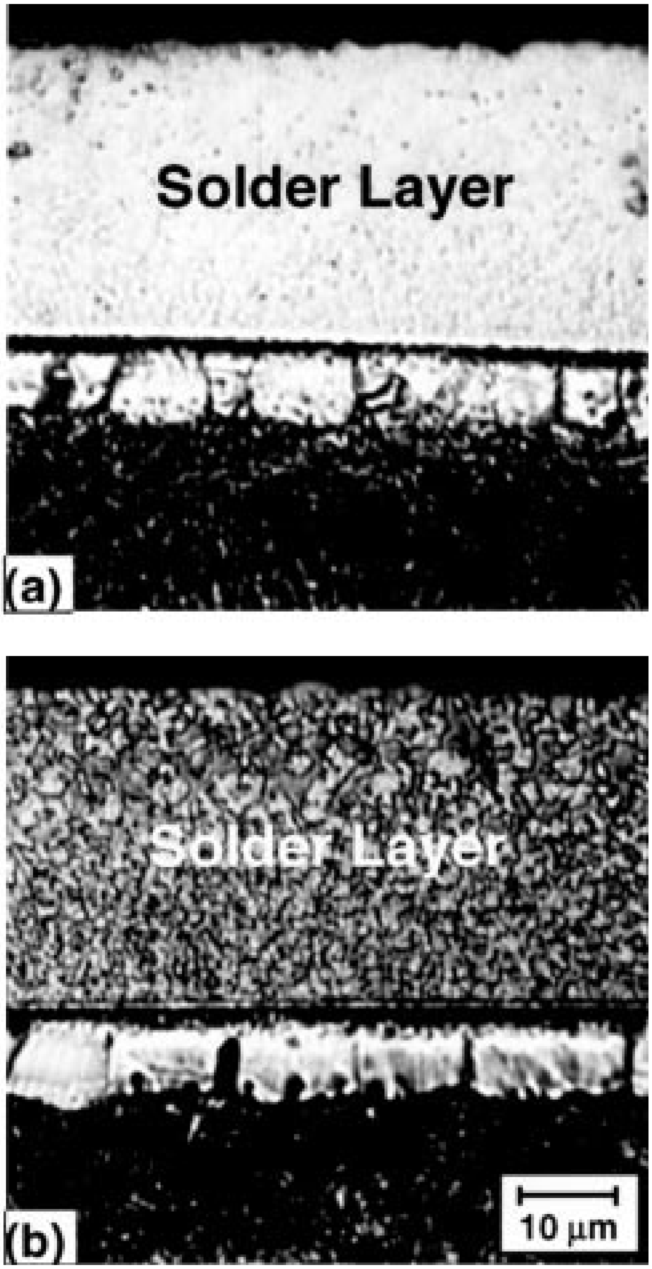

Fig. 9 Micrograph of the surface of a triple corner from an H13 mold insert showing the solder layer and the carbon-depleted region in the steel after etching with either (**a**) Vilella's reagent or (**b**) Vilella's reagent followed by Kroll's reagent

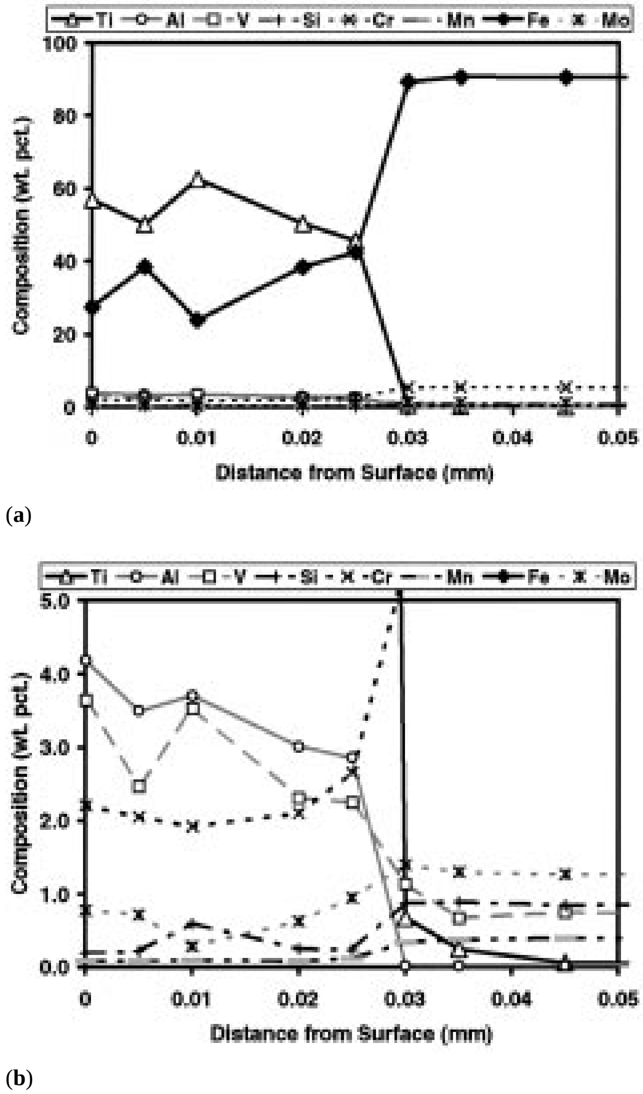

Fig. 10 WDS measurements through the solder layer developed at a triple corner of an H13 tool-steel mold insert during PMC of Ti-6Al-4V

4. Summary and Conclusions

A thorough investigation of mold wear during PMC of titanium was conducted to evaluate the relative wear resistance of three candidate mold steels and to justify this evaluation based on the observed wear types and their underlying mechanisms. The mold-material comparisons and wear-mechanism determinations were made using qualitative and quantitative results from macro- and micro-scale observations and measurements. From this work, the following conclusions were drawn.

- Soldering and "wrinkling" were the two main types of mold wear observed.
- Soldering occurred on all mold triple corners, while wrinkling occurred on select mold double corners.
- The 1040 inserts performed better than P20 or H13 inserts inasmuch as the soldered areas were smaller and wrinkling did not occur.
- Soldering is caused by the local melting of the surface of the mold due to extreme over-heating. Melted steel mixes with the liquid titanium, thereby forming a low-melting eutectic.
- Wrinkling is a result of thermal fatigue in which the thermal stresses induced during repetitive heating and cooling cause local deformation instead of cracking.
- Both soldering and wrinkling can be avoided by reducing the peak temperatures and/or the thermal gradients in the mold.

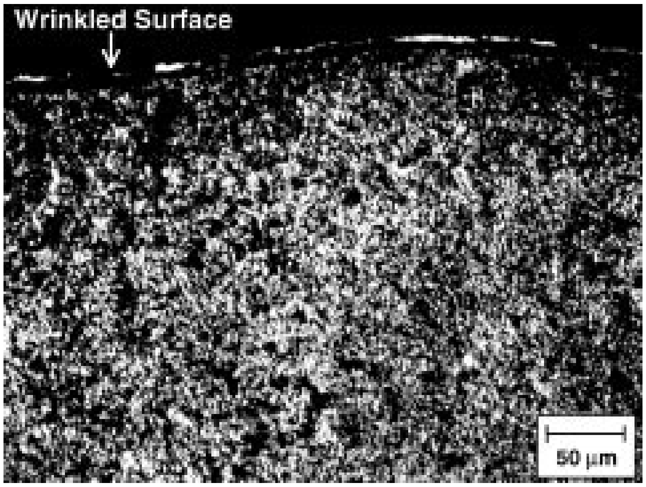

Fig. 11 Micrograph of the surface of a double corner from a P20 mold insert showing the lack of relationship between the wrinkles and the microstructure (Vilella's reagent)

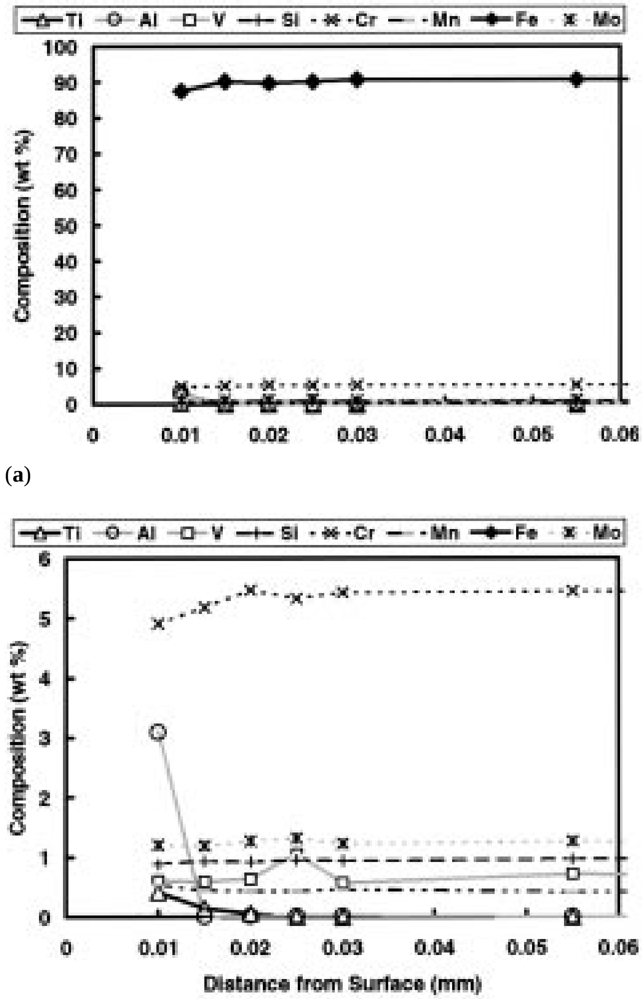

(**a**)

(**b**)

Fig. 12 WDS measurements across a double corner of an H13 tool-steel mold insert after 75 pours of Ti-6Al-4V

Acknowledgments

This work was conducted as part of the in-house research activities of the Metals Processing Group of the Air Force Research Laboratory's Materials and Manufacturing Directorate. The support and encouragement of the Laboratory management and the Air Force Office of Scientific Research (Dr. C.-S. Hartley, program manager) are gratefully acknowledged. The assistance of J. Henry, R. Lewis, and E. Fletcher in performing the experimental work is also greatly appreciated. The assistance of Howmet Corporation (G. Colvin, program manager) in performing the casting experiments and preparing the metallographic specimens is also much appreciated.

References

1. G.N. Colvin: in *Titanium '95,* P.A. Blenkinsop, W.J. Evans, and H.N. Flower, eds., Institute of Materials, London, 1996, pp. 691-701.
2. R. Shivpuri and S.L. Semiatin: "Wear of Dies and Molds in Net Shape Manufacturing," Report No. ERC/NSM-88-05, Engineering Research Center for Net Shape Manufacturing, The Ohio State University, Columbus, OH, 1988.
3. Y.-L. Chu, P.S. Cheng, and R. Shivpuri: *NADCA Int. Conf. Proc.,* NADCA, Cleveland, OH, 1993, pp. 361-71.
4. M. Sundqvist and S. Hogmark: *Tribol. Int.,* 1993, vol. 26 (2), pp. 129-34.
5. K. Venkatesan and R. Shivpuri: *J. Mater. Eng. Performance,* 1995, vol. 4 (2), pp. 166-74.
6. M. Yu, R. Shivpuri, and R.A. Rapp: *J. Mater. Eng. Performance,* 1995, vol. 4 (2), pp. 175-81.
7. P.A. Kobryn and S.L. Semiatin: "Mold-Microstructure Technique for Establishing Temperature Transients during Permanent-Mold Casting of Ti-6Al-4V," AFRL/MLLMP, Wright-Patterson AFB, OH, 2000.
8. G. Krauss: *Principles of Heat Treatment of Steel,* ASM International, Metals Park, OH, 1980.
9. H. Groot, J. Ferrier, and D.L. Taylor: "Thermophysical Properties of Three Steel Alloys," Technical Report No. TPRL 1728, Thermophysical Properties Research Laboratory, Purdue University, West Lafayette, IN, 1996.
10. J.L. Murray: in *ASM Handbook,* H. Baker, ed., ASM International, Materials Park, OH, 1992, vol. 3, pp. 2-205.
11. J.L. Murray: in *ASM Handbook,* H. Baker, ed., ASM International, Materials Park, OH, 1992, vol. 3, pp. 2-54.